Journal of Nuclear Materials 408 (2011) 18–24

Contents lists available at ScienceDirect

Journal of Nuclear Materials

journal homepage: www.elsevier.com/locate/jnucmat

Formation energy of vacancies in FeCr alloys: Dependence on Cr concentration

Emma del Rio [a,*], Jesús M. Sampedro [a], Harun Dogo [b], María J. Caturla [c], Magdalena Caro [b], Alfredo Caro [b], J. Manuel Perlado [a]

[a] Instituto de Fusión Nuclear, Universidad Politécnica de Madrid, C/José Gutiérrez Abascal, 2, 28006 Madrid, Spain
[b] Materials Science and Technology Division, MST-8, Los Alamos National Laboratory, POB 1663, Los Alamos, NM, USA
[c] Dept. de Física Aplicada, Facultad de Ciencias, Fase II, Universidad de Alicante, Alicante E-03690, Spain

ARTICLE INFO

Article history:
Received 22 September 2010
Accepted 20 October 2010

ABSTRACT

A modified version of the concentration-dependent model (CDM) potential (A. Caro et al., Phys. Rev. Lett. 95 (2005) 075702) [1] has been developed to study defects in Fe–Cr for different Cr concentrations. A comparison between this new potential and DFT results for a variety of point defect configurations is performed in order to test its reliability for radiation damage studies. The effect of Cr concentration on the vacancy formation energy in Fe–Cr alloys is analyzed in detail. This study shows a linear dependence of the vacancy formation energy on Cr concentration for values above 6% of Cr. However, the formation energy deviates from the linear interpolation in the region below 6% Cr concentration. In order to understand this behavior, the influence of the relative positions between Cr atoms and vacant sites on the vacancy formation energy has been studied.

1. Introduction

One of the key issues in the development of future fusion and generation IV fission reactors is the selection of materials [2]. Fe–Cr ferritic alloys have been identified as good candidates for structural applications in these systems due to their high resistance to swelling [3–6] and corrosion [7]. The prediction of their in-service performance under the extreme conditions characterizing these new applications, require a fundamental understanding of the changes induced by irradiation.

Computational modeling and simulations can play a significant role in studying damage production and microstructure evolution, helping in the interpretation of experimental observations, and in the extrapolation to those irradiation conditions that cannot be currently achieved experimentally [8]. For that purpose, models must provide a precise description of those defects formed under neutron irradiation and the effect that the alloying element, in this case Cr, can have on the type of defects produced as well as their migration properties. Although calculations based on density functional theory (DFT) are currently the most accurate, their high computational cost limits the system size that can be studied to point defects or small defect clusters. It is therefore necessary to develop empirical potentials that can handle calculations with thousands or millions of atoms. The accuracy of these potentials, however, must be tested against DFT results for those parameters of interest, in this case point defects.

The concentration-dependent model (CDM) is a methodology to derive potentials for complex alloys [1]. In its original application it was adjusted to the heat of formation of the Fe–Cr solid solution and was used to derive thermodynamic properties of the solution [9–11]. In this work we present a Version-2 of the potential fitted to the main features of point defects in Fe–Cr. This new potential is then used to study a large variety of defects in both bcc Fe, Cr, and Fe–Cr solutions. Results are compared with DFT calculations by Olsson et al. [12,13].

One of the important factors that require a better understanding is how the increase in Cr concentration changes the properties of the FeCr alloys. Swelling, for example, has been studied experimentally as a function of Cr content [6]. However, the correlation between macroscopic properties and microscopic structures, such as point defects, is not straightforward and it requires coupling different modeling techniques. Information of defect stabilities and binding and migration energies obtained from DFT or empirical potential calculations can be used in object kinetic Monte Carlo (OKMC) models to study defect evolution to time and length scales that can be directly compared to experimental measurements. This approach has been used very successfully in pure Fe [14–16] as well as other metals, but it is significantly more cumbersome when dealing with concentrated alloys. In these cases, understanding fundamental questions such as the dependence of defect formation energies on Cr concentration could help in the development of such OKMC models for alloys under irradiation. For that purpose,

* Corresponding author. Tel.: +34 91 336 3108; fax: +34 91 336 3002.
E-mail addresses: emma.delrio@upm.es (E. del Rio), MJ.Caturla@ua.es (M.J. Caturla), caro@lanl.gov (A. Caro).

0022-3115/$ - see front matter © 2010 Elsevier B.V. All rights reserved.
doi:10.1016/j.jnucmat.2010.10.021

we have studied in detail the dependence of the vacancy formation energy on Cr concentration.

The paper is structured as follows. In Section 2 we provide the description of the modified interatomic potential. Section 3 gives computational details. Section 4 presents the results of point defect energies (Section 4.1) and of the dependence of the vacancy formation energy on Cr concentration and distribution (Section 4.2). A summary and conclusions are presented in Section 5.

2. Composition dependent empirical potential for FeCr alloys

The Composition Dependent Model is a many body empirical potential formalism able to describe alloys with complex formation energy [1]. In its original formulation it was developed for the bcc Fe–Cr solid solution, adjusting its 0 K enthalpy of mixing to the coherent potential approximation, CPA, results of Olsson et al. [17]. In the present work, we report a new version of the potential, that we call Version-2, adjusted to additional properties in particular point defect energetics. The modifications affect the cross pair potential, which in the CDM formalism is given as a product of a function of composition times a function of distance, namely: $U_{FeCr}(x, r) = h(x) \cdot V_{FeCr}(r)$. The changes are: (i) – the polynomial h(x) has been re-fitted so that the CPA Olsson's results are reproduced by the relaxed formation energy, rather than the un-relaxed one as originally done in [1]; (ii) – the function of the distance in the cross potential $V_{FeCr}(r)$ has been modified for distances smaller than the nearest neighbor distances to properly account for the energetics of interstitials as reported by Olsson et al. [12]. These modifications do not alter any of the pure elements properties. For the alloy, predictions of properties not involving interstitials are only slightly modified with respect to the previous version.

Composition dependent potentials contain explicit 3-body terms that in principle call for a third loop on neighbors in the calculation of forces, making them appear as more computationally demanding than the standard EAM. In a recent paper [18] we show that the particular kind of 3-body forces appearing in these potentials do not require additional computational cost. The implementation of the CDM as well as tables for the present version of the Fe–Cr potential can be obtained from the Lammps website [19]. The coefficients for the $h(x)$ polynomial are given in Table 1.

3. Computational methodology

The calculations were performed at constant volume, relaxing the atomic positions by using the conjugate gradient algorithm [20]. Periodic boundary conditions were set for all the calculations. The equilibrium lattice parameter employed in the calculations of defects in Fe and Cr bcc cells are 2.855 Å and 2.878 Å respectively. The size of the cell used for the calculation of the formation energies is 2000 atoms, if not otherwise mentioned.

The definitions of formation energy and binding energies of defects used in this work are the same as those in Ref. [12] in order to compare with those DFT results. The formation energy of a given configuration, E_f, of a computational cell of N sites with nFe atoms and pCr atoms is defined as

$$E_f = \mathrm{E[nFe + pCr]} - \mathrm{nE[Fe]} - \mathrm{pE[Cr]} \quad (1)$$

where E[nFe + pCr] is the energy of the system with defects, and E[Fe] and E[Cr] are the energies per atom of the bcc Fe and bcc Cr lattices respectively. The binding energy, E_b, of a cluster of size m (where m is the number of defects) is defined as the difference between the sum of the formation energies of the isolated defects that form that cluster minus the formation energy of the cluster. The binding energy then becomes

$$E_b = \sum_{i=1,m} E_f(D_i) - E_f(\mathrm{cluster}) \quad (2)$$

where $E_f(D_i)$ is the formation energy of the defect D_i and E_f(cluster) is the formation energy of the cell with the cluster formed by the m D_i defects. Positive binding energy means attraction between the objects and reciprocally.

In order to benchmark the performance of the newly developed potential against values obtained with other available methodologies, we have calculated the formation energies of a variety of point defect configurations including vacancies and interstitials in bcc Fe and Cr lattices as well as in the solid solution. A fraction of these results have been reported previously [21].

The vacancy formation energy was calculated in a series of samples with increasing Cr concentration. Since the distance between the solute Cr atoms and the vacancy influences the formation energy of the latter, we analyzed all possible locations of the vacancy for a given sample size. Eleven samples of 1024 atoms with Cr concentrations ranging from 0.1 to 17 at.% Cr concentration were simulated using molecular dynamics at a constant temperature of 0.01 K, 0 pressure, and a run of 3000 steps with a time step of 10^{-15} seconds. Thereafter, a vacancy is added taken care that only Fe atoms were removed. At the end of the operation approximately 1000 samples (depending on the Cr concentration) were analyzed for each Cr concentration, representing all possible configurations for a given realization of the random solid solution in a 1024 atom sample.

We have also performed calculations to study the influence of the distance between the solute Cr atoms and the vacancy. We have calculated the vacancy formation energy for Fe samples with only two Cr atoms. i.e. 0.1 at.% Cr. For these calculations we have first fixed one of the Cr atoms in a 1st nearest neighbor (1nn) position with respect to the vacancy and move the other one to all possible positions from 1st nn to 5th nn to the vacancy, and then repeating these calculations fixing the 1st Cr atom at 2nn, 3nn, 4nn and 5nn positions with respect to the vacancy. Finally, we have calculated the vacancy formation energy in a bcc Fe lattice with Cr atoms placed at 1st or 2nd nn positions performing calculations over the complete set of possible configurations from 1 Cr atom up to 14 Cr.

Table 1
Values of the Redlich–Kister expansion coefficients L_p corresponding to the hof from Ref. [17] (in eV) and values of the coefficients h_i in the polynomial expression of the cross potential.

L_0	L_1	L_2	L_3	L_4
0.41566	0.0814134	−0.0101899	0.267659	−0.248269
h_0	h_1	h_2	h_3	h_4
1.05601	−0.966313	2.50521	−2.8923	1.19755

4. Results

4.1. Point defect energies in bcc Fe and bcc Cr

The point defect formation energies in pure bcc Fe using the newly developed CDM potential have been reported in a previous study [21] for a small set of defect configurations. Results in this study show that this new empirical potential reproduces the most important features in Fe–Cr alloys. In particular, the Fe–Cr mixed-interstitials are more stable than Fe–Fe or Cr–Cr interstitials for all configurations studied, that is ⟨1 1 1⟩, ⟨1 1 0⟩ and ⟨1 0 0⟩ dumbbells as well as tetrahedral and octahedral sites, as shown in Fig. 1. It is also worth noticing that the ⟨1 1 0⟩ configuration is the most stable

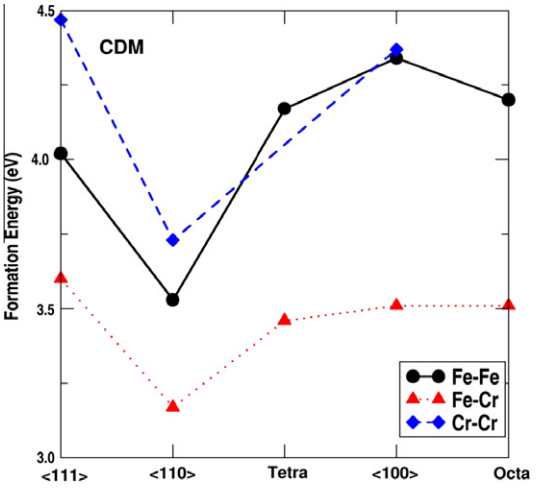

Fig. 1. Formation energies of Fe–Fe, Fe–Cr and Cr–Cr interstitials in pure bcc Fe for different configurations.

Table 2
Binding and formation energies of one and two Cr atoms with several interstitial configurations in bcc Fe. The reference energies are pure bcc Fe and pure bcc Cr, respectively. Data from Fe–Cr Version-2 CDM potential is compared to DFT calculations from reference [12].

Defect	CDM		PAW[a] (128 at.)	
	E_f (eV)	E_b (eV)	E_f (eV)	E_b (eV)
$\langle 1\,0\,0\rangle_{Fe-Cr}$	3.51	0.69	4.93	0.097
$\langle 1\,1\,0\rangle_{Fe-Cr}$	3.15	0.24	3.83	0.080
$\langle 1\,1\,1\rangle_{Fe-Cr}$	3.60	0.28	4.24	0.373
Octa-Cr	3.51	0.55	4.88	0.298
Tetra-Cr	3.46	0.57	4.26	0.074
$\langle 1\,1\,0\rangle_{Fe-Fe} \perp Cr_{subs}$	3.27	0.12	3.98	−0.065
$\langle 1\,1\,0\rangle_{Fe-Fe} - Cr_{subs}$	3.32	0.07	3.86	0.050
$\langle 1\,0\,0\rangle_{Cr-Cr}$	4.37	−0.31	5.27	−0.356
$\langle 1\,1\,0\rangle_{Cr-Cr}$	3.73	−0.48	4.23	−0.425
$\langle 1\,1\,1\rangle_{Cr-Cr}$	4.47	−0.73	4.28	0.223
$\langle 1\,1\,0\rangle_{Fe-Cr} \perp Cr_{subs}$	3.07	0.18	3.82	−0.023
$\langle 1\,1\,0\rangle_{Fe-Cr} - Cr_{subs}$	3.71	−0.46	4.01	−0.209
$\langle 1\,1\,0\rangle_{Cr-Fe} - Cr_{subs}$	3.02	0.23	3.65	0.154
$Cr_{subs} - \langle 1\,1\,0\rangle_{Fe-Fe} \perp Cr_{subs}$	3.28	−0.03	3.84	−0.041
$\langle 1\,1\,0\rangle_{Fe-Fe} - Cr_{subs}{}^{2nn}Cr_{subs}$	3.20	0.05	3.71	0.094
$\langle 1\,1\,0\rangle_{Fe-Fe} - Cr_{subs}{}^{3nn}Cr_{subs}$	3.17	0.08	3.65	0.154
$\langle 1\,1\,0\rangle_{Fe-Fe} - Cr_{subs}{}^{5nn}Cr_{subs}$	3.13	0.12	3.68	0.118
$\langle 1\,1\,0\rangle_{Fe-Fe} \perp Cr_{subs}{}^{2nn}Cr_{subs}$	3.30	−0.05	4.00	−0.195
$\langle 1\,1\,0\rangle_{Fe-Fe} \perp Cr_{subs}{}^{3nn}Cr_{subs}$	3.09	0.16	3.92	−0.121
$\langle 1\,1\,0\rangle_{Fe-Fe} \perp Cr_{subs}{}^{5nn}Cr_{subs}$	3.05	0.20	3.92	−0.123

[a] Ref. [12].

defect for all the interstitials: Fe–Fe, Fe–Cr and Cr–Cr in agreement with DFT results [12]. The calculated energy difference between the ⟨1 1 0⟩ and ⟨1 1 1⟩ configurations is 0.5 eV for the Fe–Fe interstitial as reported by other authors [22,23] and 0.45 eV for the Fe–Cr interstitial (0.41 in DFT calculations [12]).

The calculations of point defects have been extended to include multiple defects in order to evaluate the applicability of this new empirical potential for radiation damage studies. In particular we have evaluated the interactions of one and two substitutional Cr atoms with ⟨1 0 0⟩, ⟨1 1 0⟩ and ⟨1 1 1⟩ interstitials considering different possible configurations and following the DFT calculations of Olsson et al. [12]. Binding and formation energies of these interactions are presented in Table 2. Results obtained with the CDM potential are compared to those obtained from DFT calculations [12]. Fig. 2 displays all the configurations studied in Table 2. There are significant qualitative, and in some cases, quantitative agreements with the DFT results in terms of binding energies and relative stabilities of defects despite the fact that the interatomic potential has not been fitted explicitly to any of these configurations.

For the mixed-interstitials (Fig. 2a–e), as discussed above, the most stable configuration is the ⟨1 1 0⟩ dumbbell both in DFT and in the empirical potential, and in all cases there is a positive binding like in DFT. The binding energy of the ⟨1 1 0⟩ dumbbell obtained from the CDM potential is higher than the DFT value, 0.24 eV and 0.08 eV respectively, and the largest discrepancy is for the $\langle 1\,0\,0\rangle_{Fe-Cr}$ configuration, with a binding energy of 0.69 eV in contrast with DFT results where this binding energy is very small (0.097 eV).

Interaction of Cr in the tensile, $\langle 1\,1\,0\rangle_{Fe-Fe} \perp$ Cr, and compression, $\langle 1\,1\,0\rangle_{Fe-Fe}$ – Cr, sites with ⟨1 1 0⟩ Fe–Fe interstitial (Fig. 2f and g, respectively) are small, slightly attractive in the case of the CDM potential with a higher value for the tension site (0.12 and 0.07 eV, respectively). These results differ from DFT where the interaction is repulsive with a Cr in the tensile site (−0.065 eV) and positive (0.05 eV) in the other case.

The binding energy of two Cr atoms forming a ⟨1 0 0⟩ interstitial, $\langle 1\,0\,0\rangle_{Cr-Cr}$, becomes negative (repulsion), (−0.31 eV with the CDM-Version 2 potential and −0.356 eV in DFT calculations) in agreement with DFT results (Fig. 2h in contrast with Fig. 2a). The same occurs for the $\langle 1\,1\,0\rangle_{Cr-Cr}$ interstitial (Fig. 2i in contrast with Fig. 2b), namely negative binding energy and very similar to the DFT results (−0.48 eV for the CDM-Version 2 potential and −0.425 eV for DFT).

For one Cr atom and a mixed $\langle 1\,1\,0\rangle_{Cr-Fe}$ dumbbell (Fig. 2k–m) the most stable configuration is $\langle 1\,1\,0\rangle_{Cr-Fe} - Cr_{subs}$, Fig. 2m, for the CDM potential with a binding energy of 0.23 eV, in good agreement with DFT calculations (0.154 eV). The CDM binding energies reflect a dependence on the distance between the two Cr atoms being negative when the Cr atoms are close to each other, where the small distance allows the Cr-pair repulsion to dominate over the attraction present for the single-Cr configurations, increasing to positive values as the distance between these atoms increases. This agrees with the observations of repulsion between Cr atoms in Fe by Klaver et al. [24].

The interaction between Cr in substitutional sites and a ⟨1 1 0⟩ Fe–Fe interstitial has also been studied for different configurations (Fig. 2n–t). Of these different configurations, only two have the opposite sign with respect to the DFT results, namely configurations in Fig. 2s and t where the CDM potential predicts an attraction and the DFT results show a repulsion although with small binding energies (−0.1 eV).

Defects in bcc Cr have also been studied, including ⟨1 0 0⟩, ⟨1 1 0⟩ and ⟨1 1 1⟩ Fe–Fe and Fe–Cr interstitials and results are presented in Table 3. As shown in Fig. 3 (for comparison with Fig. 1), the most stable configuration for all cases is the ⟨1 1 0⟩ dumbbell, as in the case of a bcc Fe matrix. However, in the case of the Fe–Cr mixed-interstitials the energy difference between the ⟨1 1 0⟩ dumbbell and the ⟨1 0 0⟩ configuration is almost negligible. This is also the case between the ⟨1 1 0⟩ and ⟨1 1 1⟩ Cr–Cr self-interstitials and in agreement with DFT results, as mentioned above. Notice that the Fe–Cr and Fe–Fe interstitial formation energies in chromium are more than 1 eV smaller than Cr–Cr self-interstitial formation energies and have the same order of magnitude than these interstitials in iron.

4.2. Dependence of the vacancy formation energy on Cr concentration and distribution

We have applied the new empirical potential to the study of the vacancy formation energy in bcc Fe–Cr random solid solution as a function of Cr concentration. Calculations were performed for 11 different Cr concentrations ranging between 0.1 and 17 at.% Cr.

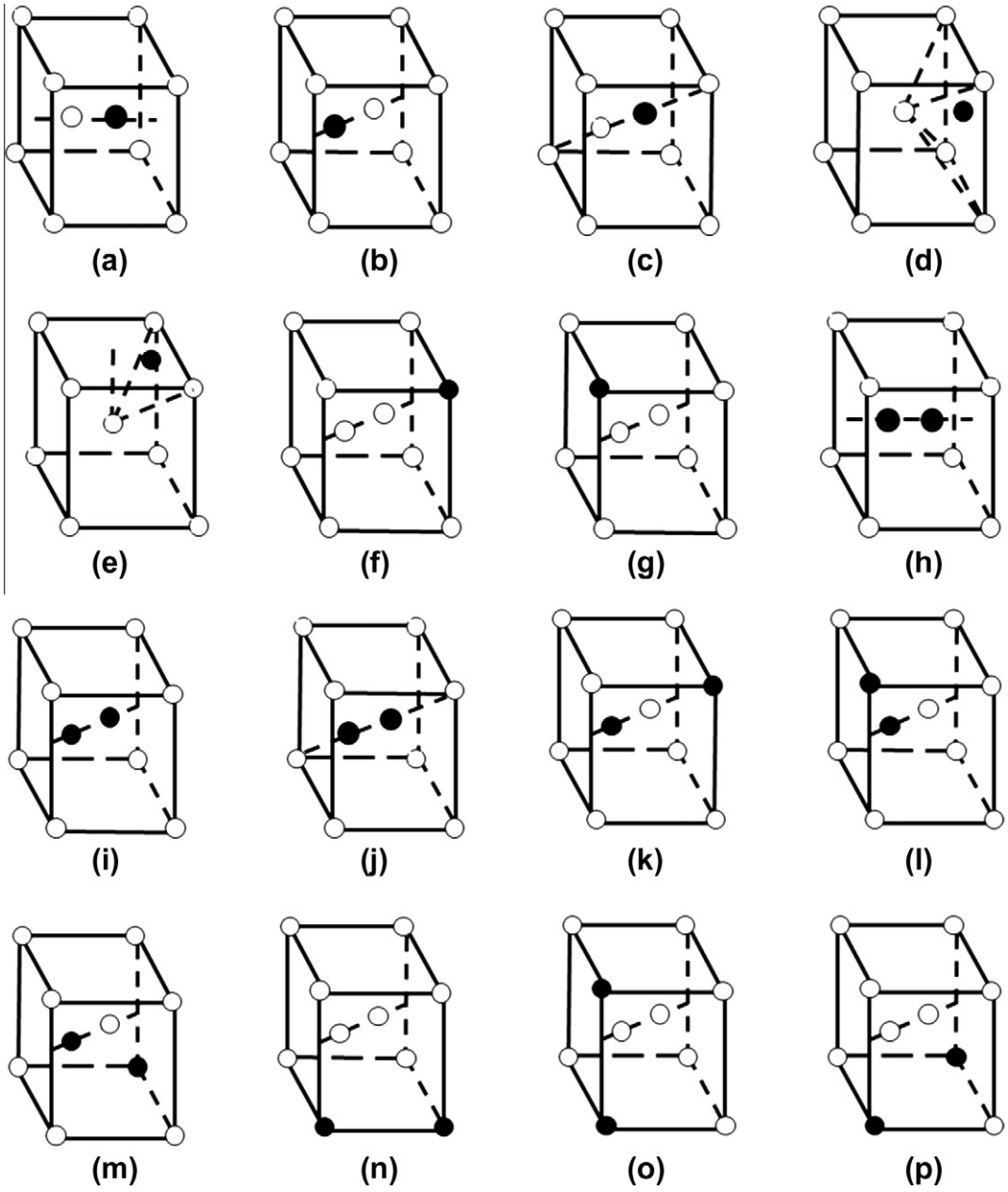

Fig. 2. SIA – Cr and SIA – two Cr configurations: (a) Fe–Cr ⟨1 0 0⟩ dumbbell ($\langle 1\,0\,0\rangle_{Fe-Cr}$), (b) Fe–Cr ⟨1 1 0⟩ dumbbell ($\langle 1\,1\,0\rangle_{Fe-Cr}$), (c) Fe–Cr ⟨1 1 1⟩ dumbbell ($\langle 1\,1\,1\rangle_{Fe-Cr}$), (d) Fe–Cr octahedral interstitial, (e) Fe–Cr tetrahedral interstitial, (f) Cr near ⟨1 1 0⟩ dumbbell at the site under tension ($\langle 1\,1\,0\rangle_{Fe-Fe} \perp Cr_{subs}$), (g) Cr near ⟨1 10⟩ dumbbell at the site under compression ($\langle 1\,1\,0\rangle_{Fe-Fe} - Cr_{subs}$), (h) Cr substituted ⟨1 0 0⟩ dumbbell ($\langle 1\,0\,0\rangle_{Cr-Cr}$), (i) Cr substituted ⟨1 1 0⟩ dumbbell ($\langle 1\,1\,0\rangle_{Cr-Cr}$), (j) Cr substituted ⟨1 1 1⟩ dumbbell ($\langle 1\,1\,1\rangle_{Cr-Cr}$), (k) Mixed ⟨1 1 0⟩ dumbbell and Cr in the tension site ($\langle 1\,1\,0\rangle_{Fe-Cr} \perp Cr_{subs}$), (l) mixed ⟨1 1 0⟩ dumbbell and Cr in the near compression site ($\langle 1\,1\,0\rangle_{Fe-Cr} - Cr_{subs}$), (m) mixed ⟨1 1 0⟩ dumbbell and Cr in the far compression site ($\langle 1\,1\,0\rangle_{Cr-Fe} - Cr_{subs}$), (n) one Cr in compression site and one in tension site around ⟨1 1 0⟩ dumbbell ($Cr_{subs} - \langle 1\,1\,0\rangle_{Fe-Fe} \perp Cr_{subs}$), (o) two Cr in 2nn compression sites in front of a ⟨1 1 0⟩ dumbbell ($\langle 1\,1\,0\rangle_{Fe-Fe} - Cr_{subs}{}^{2nn}Cr_{subs}$), (p) two Cr in 3nn compression sites around ⟨1 1 0⟩ dumbbell ($\langle 1\,1\,0\rangle_{Fe-Fe} - Cr_{subs}{}^{3nn}Cr_{subs}$), (q) two Cr in 5nn compression sites around ⟨1 1 0⟩ dumbbell ($\langle 1\,1\,0\rangle_{Fe-Fe} - Cr_{subs}{}^{5nn}Cr_{subs}$), (r) two Cr in 2nn tension sites around ⟨1 1 0⟩ dumbbell ($\langle 1\,1\,0\rangle_{Fe-Fe} \perp Cr_{subs}{}^{2nn}Cr_{subs}$), (s) two Cr in 3nn tension sites around ⟨1 1 0⟩ dumbbell ($\langle 1\,1\,0\rangle_{Fe-Fe} \perp Cr_{subs}{}^{3nn}Cr_{subs}$) and (t) two Cr in 5nn tension sites around ⟨1 1 0⟩ dumbbell ($\langle 1\,1\,0\rangle_{Fe-Fe} \perp Cr_{subs}{}^{5nn}Cr_{subs}$). The Cr position is indicated by the black circle.

The solid solution is thermodynamically unstable for concentrations above ~10% but these static or low temperature calculations do not allow for precipitation to occur. All calculations were performed in 1024 atom cells. For each sample we have performed calculations over the entire ensemble of possible configuration, that is removing an atom at every one of the 1024 lattice sites. A histogram of energies was produced for each set of samples containing the same number of Cr atoms (see Fig. 4), and a Gaussian distribution function was fitted to it, providing mean energy and standard deviation. Each mean value for total enthalpy of a sample including a vacancy was then used in conjunction with the respective value of total enthalpy of the same sample without the vacancy to provide the formation energy of the vacancy and its dispersion at the given Cr concentration, as shown in Fig. 5.

We can observe that dispersions are larger at high Cr concentration. Fig. 5 shows some interesting results. In an ideal solution the vacancy formation energy would follow a direct interpolation between the pure element values. However, the formation energy in Fig. 5 deviates from the linear interpolation in the region below 6% Cr concentration, similar to the behavior of the heat of

Table 3
Point defect formation energy (eV) of vacancies and interstitials in pure bcc Cr including ⟨1 0 0⟩, ⟨1 1 0⟩ and ⟨1 1 1⟩ Fe–Cr, Fe–Fe and Cr–Cr interstitial configurations. All calculations performed with cell size of 1024 atoms, except for the Cr–Cr interstitials, performed with 2000 atoms.

Defect	E_f (eV) CDM	PAW[a] NM (128 atoms)	PAW[a] AF (128 atoms)	PLATO[b] (128 atoms)
$\langle 1\,0\,0\rangle_{Fe-Cr}$	3.73			
$\langle 1\,1\,0\rangle_{Fe-Cr}$	3.72			
$\langle 1\,1\,1\rangle_{Fe-Cr}$	4.14			
$\langle 1\,0\,0\rangle_{Fe-Fe}$	3.83			
$\langle 1\,1\,0\rangle_{Fe-Fe}$	3.54			
$\langle 1\,1\,1\rangle_{Fe-Fe}$	4.10			
$\langle 1\,0\,0\rangle_{Cr-Cr}$	6.84	6.75	6.71	6.643
$\langle 1\,1\,0\rangle_{Cr-Cr}$	5.60	5.62	5.66	5.674
$\langle 1\,1\,1\rangle_{Cr-Cr}$	5.62	5.63	5.70	5.685
Octahedral	7.07	6.78	6.73	6.723
Tetrahedral	6.50	6.35	6.31	6.189
Vacancy	2.56	2.61	2.71	2.64

[a] Ref. [12].
[b] Ref. [13].

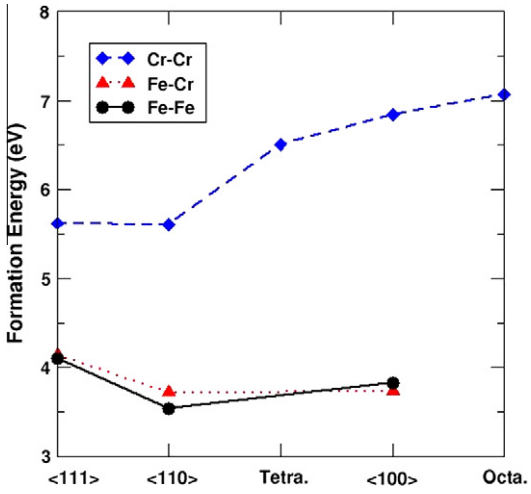

Fig. 3. Formation energies of Fe–Fe, Fe–Cr and Cr–Cr interstitials in pure bcc Cr for different configurations.

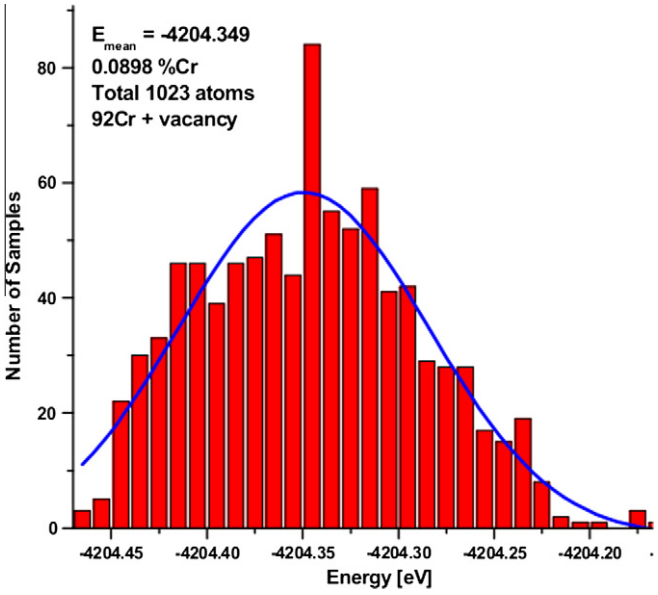

Fig. 4. Histogram of the energy distribution in a sample with 0.0898% Cr and one vacancy, together with a Gaussian fit.

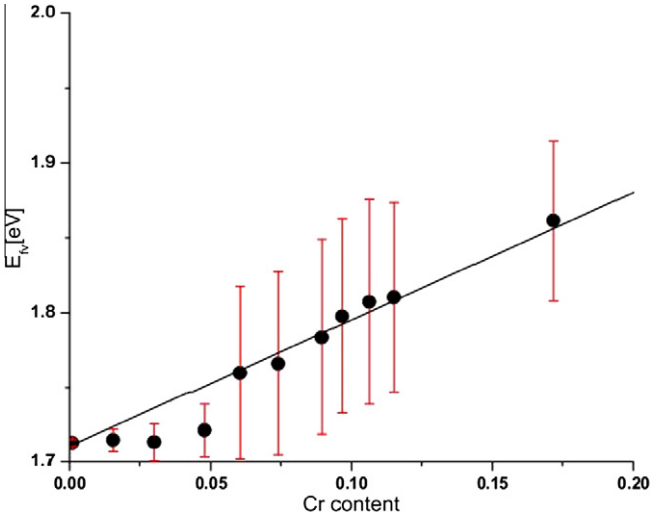

Fig. 5. Vacancy formation energy and dispersion as a function of Cr content.

formation of the alloy. Additionally, an increase in the Cr concentration translates into an increase in the number of different possible configurations and consequently in the spread of values, since we have more possibilities of finding the Cr atoms in different positions with respect to the vacancy.

In order to study the influence of the distance between the solute Cr atoms and the vacant sites, calculations on the vacancy formation energy with particular positions of the Cr atoms have been performed. Firstly, we have calculated the maximum and minimum values for each concentration for four different and random Cr distributions, as shown in Fig. 6. As mentioned above, one would expect the maxima and minima values to increase linearly with the concentration. In contrast, Fig. 6 shows that minima values are almost constant with the increasing concentration and almost equal to the value of the vacancy formation energy in pure iron, whereas maxima values increase with the Cr concentration in steps. Nevertheless, we can observe in this figure how the dispersion in the values increases with the Cr concentration, just as shown before in Fig. 5.

It is already known from DFT calculations [12] that the presence of a single Cr atom does not influence the vacancy formation energy, even if the Cr atom is first nearest neighbor to the vacant site. Therefore, to study further the correlation between the Cr atoms

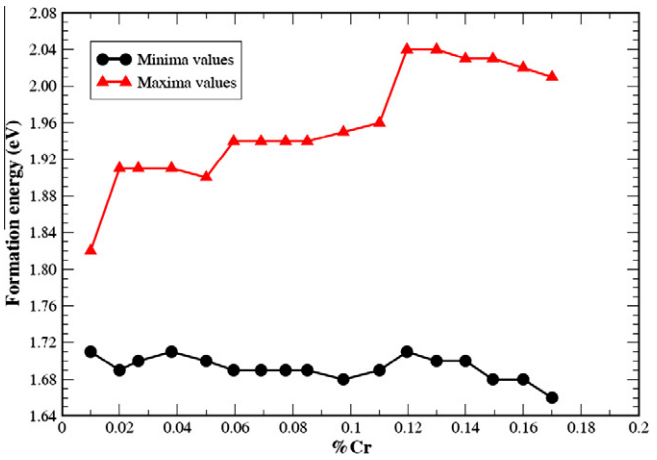

Fig. 6. Minimum and maximum values of the vacancy formation energy as a function of Cr content for random FeCr solid solutions.

Table 4
Vacancy formation energy in a bcc Fe lattice when 2 Fe atoms have been substituted by Cr atoms. First and second columns indicate the relative position of the Cr atoms with respect to the vacancy.

Cr_1	Cr_2	E_{fv} (eV)
2	2	1.92
1	1	1.87
1	2	1.87
2	4	1.81
2	5	1.81
2	3	1.80
1	4	1.78
1	5	1.77
1	3	1.76
4	4	1.70
4	5	1.70
5	5	1.70
3	5	1.69
3	4	1.68
3	3	1.67

and the vacant site we have performed calculations in Fe with one vacancy and two substitutional Cr atoms in different positions with respect to the vacancy and with respect to each other. We fixed one Cr atom in a first nearest neighbor (1nn) position with respect to the vacancy and moved the second Cr atom from 1nn to 5nn position. We have repeated these calculations with one Cr atom fixed at 2nn and the other Cr atom moving from 2nn to 5nn and so on, with the first Cr atom up to 5nn position. Results are presented in Table 4. Analyzing these results we can observe three different value ranges for the vacancy formation energies. There is one value which is almost equal to the value for the vacancy formation energy in iron (1.7 eV), and that is obtained when the two Cr atoms are further away than the 2nn position with respect to the vacancy. There is another set of values slightly higher than the first set and that is obtained when only one of the two Cr atoms is at 1nn or 2nn position. And finally a third set of values with the highest vacancy formation energy when the two Cr atoms are in 1nn or 2nn positions with respect to the vacancy. It is interesting to note that the value is higher when the two Cr atoms are at 2nn positions from the vacancy than when they are both located at 1st nn position, showing the influence of the repulsion between Cr atoms. These results imply that at least two Cr atoms must be closer than 2nn position in order to observe a significant difference in the vacancy formation energy. This could explain the behavior of the average vacancy formation energy as a function of Cr content shown in Fig. 4, where for concentrations less than 6% the vacancy formation energy is almost constant, since the probability of having two Cr atoms close to the vacancy at these concentrations is quite low. In fact, the probability of having n atoms of the alloying element as first nearest neighbors in a bcc lattice for a given concentration c can be obtained from the binomial distribution:

$$P[n,c] = \frac{8!}{[8-n]!n!} c^n [1-c]^{8-n} \quad (3)$$

Using this function Fig. 7 shows the probability of a vacancy having more than one Cr atom at first nearest neighbor distance as a function of Cr concentration. It is clear from this figure that this probability is highly non-linear at low composition, below about 7%, effect that explains the similar behavior for the formation energy of a vacancy reported in Fig. 5. In general, these results show a dependence of the vacancy formation energy on the Cr local concentration increasing with Cr atoms at 1nn or 2nn positions, but not being affected when the Cr atoms are further away from these positions.

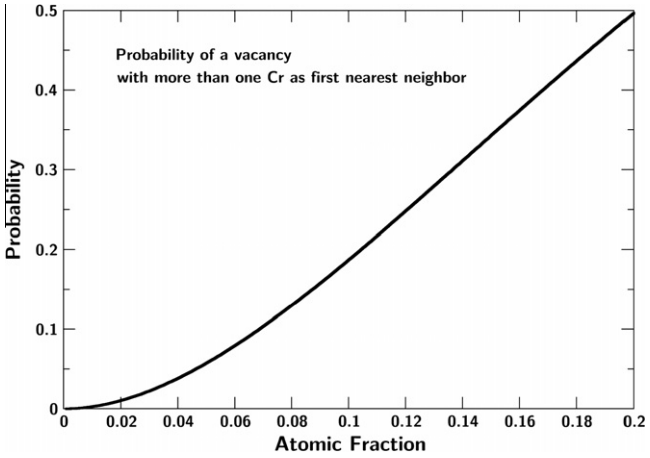

Fig. 7. Probability of having more than one Cr atom at first nearest neighbor distance of a vacancy as a function of Cr concentration in FeCr random solution.

To confirm these observations, we have performed calculations on the vacancy formation energy as a function of the number of Cr atoms at 1nn or 2nn positions. We have calculated all the possible configurations when we have one Cr atom at 1nn or 2nn position and increasing the number of Cr atoms up to 14 (8 atoms at 1nn and 6 atoms at 2nn positions). Fig. 8 represents the maxima and minima values of the vacancy formation energy as a function of the number of Cr atoms. In this case maxima and minima values increase almost linearly with the number of Cr atoms at 1nn or 2nn positions. We can also observe that the vacancy formation energy increases from 1.7 eV when there is no Cr atom at 1nn or 2nn positions to 2.25 eV when all the 14 Cr atoms are at 1nn and 2nn. Note that the vacancy formation energy in Cr is 2.56 eV [21]. We conclude then that the influence of the chemical nature of neighbors beyond the second coordination shell contributes with only ~10% to the total vacancy formation energy.

To check these findings, we analyzed the local Cr distribution around the vacancy for the four random distributions studied as a function of Cr content. We observed that all those configurations with vacancy formation energy equal to pure Fe do not have any Cr atom at 1st or 2nd nearest neighbors, and complementary, configurations showing an increase of the vacancy formation energy, have at least one Cr atom sits as 1nn or 2nn. All these findings are in good agreement with some experimental and DFT calculations performed by Froideval et al. [25] where they find that

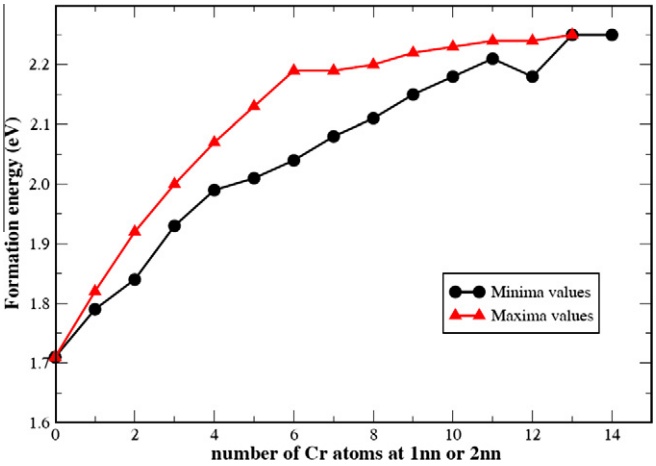

Fig. 8. Vacancy formation energy as a function of the number of Cr atoms at 1nn or 2nn positions.

the alloy composition strongly influences the Cr local structure. They have also observed changes in the magnetic and structural properties of FeCr alloys with the Cr content with a distance contraction in the two first shells around the Cr atom.

5. Summary and conclusions

We present a new version of the CDM potential for Fe–Cr, adequate to describe point defects in ferritic steels. A detailed comparison between DFT and classical results tests the validity of this classical approach. We have calculated formation energies for Fe–Fe and mixed Fe–Cr interstitials in bcc Cr and formation and binding energies between one or two Cr atoms with $\langle 1\,0\,0\rangle$, $\langle 1\,1\,0\rangle$ and $\langle 1\,1\,1\rangle$ interstitials in bcc Fe for several configurations. These calculations, and in particular the stability of the mixed Fe–Cr interstitials with respect to all other configurations studied, show an overall reasonable agreement with ab initio results. Also, $\langle 1\,1\,0\rangle$ configurations are the most stable for Fe–Fe, Fe–Cr and Cr–Cr interstitials and the strong Cr–Cr repulsion in the dilute limit is properly captured, although this repulsion is slightly overestimated especially for the $\langle 1\,1\,1\rangle_{Cr-Cr}$ dumbbell.

DFT and experimental studies indicate that the magnetic structure of the FeCr alloys is critical in determining its energetics [12,25]. The ability to model these properties with classical potentials is a subject that has captured significant attention in recent years. The particular empirical potential used in this work does not contain any explicit degree of freedom of magnetic origin, therefore it can only provide a qualitative description of the Fe–Cr system. For example, it shows a strong repulsion when two or more substitutional Cr atoms are nearby.

We have also studied the vacancy formation energy using the empirical potential developed. Despite the fact that the interaction between Cr and vacancies is expected to be weak, we can observe a dependence of the formation energy of vacancies as a function of Cr concentration. For concentrations above 6%, the values obtained show a linear dependence with the concentration between the vacancy formation energy in iron (1.72 eV) and the vacancy formation energy in chromium (2.56 eV). However, for concentrations below 6 at.% Cr the vacancy formation energy is almost constant. The dispersion in values below 6% is small and it increases with increasing Cr concentration reflecting the higher probability of having more than one Cr atom close to the vacant site.

Finally, we have performed some calculations to study the dependence of the formation energy with the local distribution of Cr atoms. From these calculations, we conclude that if Cr atoms are further away than 2nd nearest neighbor position with respect to the vacancy they have a small effect on the formation energy value. This could explain the constant formation energy value for low Cr concentrations as there is a small probability of finding Cr atoms at 1nn or 2nn positions with respect to the vacancy, and the mean energy value obtained over the entire ensemble of possible configurations remains constant. In contrast, if Cr atoms are positioned at first or second nearest neighbor with respect to the vacancy, its formation energy increases. Therefore the Cr concentration has to be high enough in order to have a high probability of finding a Cr atom at 1nn or 2nn positions to show any effect in the energy. We have calculated the extreme case where all the 1st and 2nd nearest neighbor positions are occupied with chromium atoms, the rest being Fe, and the value obtained is close to that of the vacancy in a Cr bcc sample.

Acknowledgements

We thank Lorenzo Malerba and Pär Olsson for valuable discussions. This work has been partially supported by the European Commission within the FP7 project GETMAT (Grant agreement number 212175), the VI Spanish National Project ENE2008-06403-C06-06, the European Union Keep in Touch Program on Inertial Confinement Fusion (ref. 08/061), and the European Fusion Development Agreement (EFDA). Alfredo Caro was supported by the Center for Materials at Irradiation and Mechanical Extremes, an Energy Frontier Research Center funded by the US Department of Energy (Award Number 2008LANL1026) at Los Alamos National Laboratory. This work also contributes to the International Atomic Energy Agency CRP SMoRE program.

References

[1] A. Caro, D.A. Crowson, M. Caro, Phys. Rev. Lett. 95 (2005) 075702 (See also); B. Sadigh, P. Erhart, A. Stukowski, A. Caro, Philos. Mag. 89 (2009) 3371.
[2] B. van der Schaaf, E. Diegele, R. Laesser, A. Moeslang, Fusion Eng. Des. 81 (2006) 893.
[3] M.L. Jenkins, C.A. English, B.L. Eyre, Philos. Mag. A 38 (1978) 97.
[4] E.A. Little, D.A. Stow, J. Nucl. Mater. 87 (1979) 25.
[5] E.A. Little, R. Bullough, M.H. Wood, Proc. R. Soc. London A (1980) 372.
[6] F.A. Garner, M.B. Toloczko, B.H. Sencer, J. Nucl. Mater. 276 (2000) 123.
[7] A. Fry, S. Osgerby, M. Wright, Oxidation of Alloys in Steam Environment – A Review, National Physics Laboratory Report NPL MATC(A), 2002, p. 90.
[8] S.L. Dudarev et al., J. Nucl. Mater. (2009) 386–388.
[9] A. Caro, M. Caro, E.M. Lopasso, Appl. Phys. Lett. 89 (2006) 21902.
[10] A. Caro, M. Caro, P. Klaver, B. Sadigh, E.M. Lopasso, S.G. Srinivasan, J. Min. Met. Mater. (JOM) 59 (April) (2007) 2.
[11] P. Erhart, A. Caro, M. Caro, B. Sadigh, Phys. Rev. B 77 (2008) 134206.
[12] P. Olsson, C. Domain, J. Wallenius, Phys. Rev. B 75 (2007) 014110.
[13] D. Nguyen-Manh, S.L. Dudarev, A.P. Horsfield, J. Nucl. Mater. 367 (2007) 257.
[14] C.C. Fu, J. Dalla Torre, F. Willaime, J.L. Bocquet, A. Barbu, Nature Mater. 4 (2005) 68.
[15] N. Soneda, S. Ishino, A. Takahashi, K. Dohi, J. Nucl. Mater. 323 (2003) 169.
[16] C. Domain, C.S. Becquart, L. Malerba, J. Nucl. Mater. 335 (2004) 121.
[17] P. Olsson, I.A. Abrikosov, L. Vitos, J. Wallenius, J. Nucl. Mater. 321 (2003) 84.
[18] A. Stukowski, B. Sadigh, P. Erhart, A. Caro, Modell. Simul. Mater. Sci. Eng. 17 (2009) 075005.
[19] <http://lammps.sandia.gov>, <http://www.mm.mw.tu-darmstadt.de/~stuko/cdeam/index.html>.
[20] Numerical Recipes in Fortran 77, second ed., 1992, p. 413.
[21] J.M. Sampedro, E. del Río, M.J. Caturla, M. Victoria, J.M. Perlado, Proceedings of 14th International Conference on Fusion Reactor Materials (ICFRM-14), Sapporo (Japan), September 2009, J. Nucl. Mater.
[22] F. Willaime, C.-C. Fu, M.C. Marinica, J. Della Torre, Nucl. Instrum. Methods Phys. Res. B 228 (2005) 92–99.
[23] D. Terentyev, L. Malerba, M. Hou, Phys. Rev. B 75 (2007) 104108.
[24] T.P.C. Klaver, R. Drautz, M.W. Finnis, Phys. Rev. B 74 (2006) 094435.
[25] A. Froideval, R. Iglesias, M. Samaras, S. Schuppler, P. Nagel, D. Grolimund, M. Victoria, W. Hoffelner, Phys. Rev. Lett. 99 (2007) 237201.